Shaking Table Model Tests on Dynamic Structure-Soil-Structure Interaction during Various Excitations

P.Z. Li, X.Y. Hou, Y.M. Liu & X.L. Lu
State Key Laboratory of Disaster Reduction in Civil Engineering, Tongji University, P. R. China

15 WCEE
LISBOA 2012

SUMMARY:
Shaking table model tests on dynamic structure-soil-structure interaction during various excitations were conducted. A flexible container was fabricated to minimize the boundary effects. The tests adopted uniform silt clay as the model soil, 12-story cast-in-place reinforced concrete frames as the superstructures, and 3 by 3 group piles as the foundations. The model scale was 1/15. The El Centro wave and Shanghai bedrock wave were adopted as excitations. Test results show that the seismic damage of adjacent high-rise buildings due to natural earthquake was reproduced well. Some important findings from the tests are as follows. The adjacent structures would damage more serious than that in single one. The dynamic response of the SSSI system, the strain response of piles and contact pressure between the surfaces of the pile-soil are influenced by the SSSI effect.

Keywords: structure-soil-structure interaction; shaking table test; dynamic characteristics; seismic response

1. INTRODUCTION

In the recent decades, the city blocks that contain clusters of closely spaced buildings have come forth in the world. During earthquake events, the radiation energy would be emitted from a vibrating structure to other structures through the soil. There will have influence on the dynamic characteristics and the earthquake response among the closed spaced buildings, which calls Structure-Soil-Structure Interaction (SSSI). Notably, for structures located in dense urban environments composed of the city blocks, the assumption of buildings being isolated from each other is invalid, and can lead to erroneous results. Therefore, consideration of the interaction of soil, foundations, and structures requires a more holistic approach. Study on the SSSI is of great importance to predicting the seismic responses of structure exactly and have become a hotspot in the fields of earthquake engineering research.

Some interrelated research has received much attention in the theoretical studies and numerical analysis. For example, Qian and Beskos (1995) developed a boundary element method (BEM) model for considering interaction between adjacent, massless foundations. Mulliken and Karabalis (1998) developed a lumped mass model to consider ground-motion induced interactions between adjacent, massless foundations. Lehmann and Antes (2001) developed a numerical, hybrid model to investigate the dynamic interaction systems submitted to time-harmonic loads. Yahyai et al. (2008) used ANSYS program to simulate two steel moment frames with concrete shear walls on three types of soil. Padron et al. (2009) utilized FEM-BEM method in frequency domain to analyze including pile foundations. Besides, some experiment and field observation also have been conducted. Mizuno (1980) clarified actual phenomena of the SSSI by a series of experiments such as forced vibration tests and earthquake observations for a full-scale building and a model structure. The Nuclear Power Engineering Corporation (NUPEC) carried out forced vibration tests and shaking table tests using models of reactor buildings and adjacent structures from 1994 to 2002 (e.g., Nakagawa et al. 1998, Kitada et al. 1999). As part of a collaborative program, Xu (2004) and Broc (2006) make calculation study on the tests using the SASSI program and FEM-BEM method. Celebi (1993) analyzed the data from two adjacent 16.3m seven layers steel structure and the soil which is the certain depth from the basement of a structure nearby in the Whittier Narrows earthquake in the United States. More recently, some work have been done on analyzing the influence of large groups of buildings, as well as that of site effects due to subsoil configuration, on the seismic response of the overall system by means of several experimental and numerical models (e.g., Gueguen et al. 2002, Groby et al. 2005, Bard et al. 2006, Kham et al. 2006, Semblat et al. 2008, Ghergu et al. 2009).

However, limited by facilities and cost, current studies have been mostly focused on theoretical study and calculation analysis, and little experimental work has been conducted. Actually, many theoretical outcomes were difficult to guide practical engineering due to the lack of test validation. The experimental study on the SSSI system is very significant.

Under the sponsorship of the National Natural Science Foundation of China, the shaking table tests on the Soil-Structure Interaction (SSI) system and SSSI system have been conducted in the State Key Laboratory of Disaster Reduction in Civil Engineering of Tongji University. The dynamic responses of soil and structures during earthquake shakings were documented by accelerometers, displacement meters and strain gauges, attached to the structures and embedded in the soils surrounding the structures. This paper would give the results from the shaking table tests.

2. DESCRIPTION OF SHAKING TABLE MODEL TEST

The shaking table tests had been completed in 2010. The SSSI effect was measured by adopting two models (PS15S and PS15C) in the tests, one including only single structure (Fig. 1) and the other including two adjacent structures with closed spaced (Fig. 2).

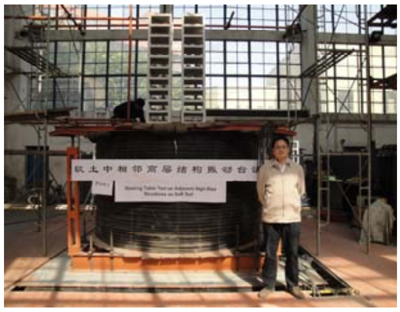

Figure 1. PS15S test model **Figure 2.** PS15C test model
(Note: PS - Pile Structure; 15 - 1/15 scale; S - Single; C - Cross)

The structural models represented a 12-story cast-in-place reinforced concrete frame with 3 by 3 pile group foundation. The tests adopted uniform silt clay as the model soil, and a flexible cylindrical container was used to reduce the undesirable boundary effects.

2.1. Simulation of Soil Boundary Conditions

In the shaking table test, a flexible container was used to reduce the undesirable boundary effects (Fig. 3). The flexible container used herein was cylindrical and 3000 mm in diameter. Its lateral rubber membrane was 5 mm thick. In order to provide radial rigidity and permit soil to deform as horizontal shear layer, the container was reinforced in the tangential direction with steel loops 4 mm in diameter, spaced by 60 mm (Lu et al., 2002b; Li et al., 2008). Each reinforcement loop was made of steel bar by weld. The lateral side of the cylinder was fixed with the upper ring plate and the base plate by bolt. Four columns fixed on the base plate support the upper ring plate. A universal joint was installed on each column top to enable the ring plate to displace laterally, so the four columns had no restraint to the container in horizontal direction. Height adjustable screw rod was installed on the column to adjust the upper plate to horizontality and to adjust the cylinder to a proper state. The base plate was made of steel plate, and stiffened with small steel beams to avoid over-deformation during lifting. In order to minimize relative slippage between the soil and the container on the base surface, a crushed rock was bonded to the base steel plate by epoxy resin to make the surface rough.

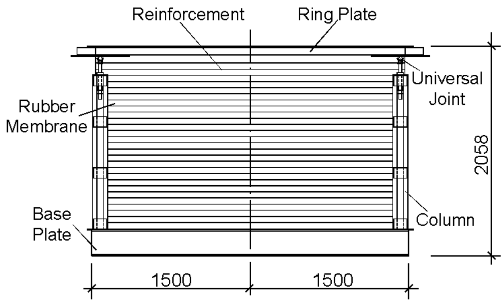

Figure 3. Side view of the flexible container

2.2. Similitude Model Design

Owing to the limit of the shaking table, the size of the SSI and SSSI models in the test was scaled down from full-scale buildings and foundations. The test models used similitude principles and practical considerations commonly used in the seismic study of SSI systems in shaking table tests (Lu et al., 2002a; Lu et al., 2005). Similar relations were applied to soil, foundation and superstructure, but the effects of earth gravity were not scaled. Besides, extra weights were not added in the present study.

All physical quantities in the test were scaled using similitude formulas from the Bockingham π theorem. Table 1 provides a summary of important scale factors for the shaking table tests.

Table 1. Similar Relationship of the Tests

Physical Quality	Model Dimension/ Prototype Dimension	Physical Quality	Model Dimension/ Prototype Dimension
Strain	1	Area Load	1/4.556
Elastic Modulus	1/4.556	Mass	1/3375
Density	1	Time	0.1423
Length	1/15	Velocity	0.4685
Linear Displacement	1/15	Acceleration	3.2924
Concentrated Force	1/1025	---	---

2.3 Design of the Models

The superstructures were 12-story reinforced concrete frames, with a single bay and a single span. There had a single superstructure in the PS15S test model and two same superstructures in the PS15C test model. The clear distance between the two superstructures in the PC15C test was equal to half of the width of the superstructure (i.e. it was 200 mm). The silt clay was used for the model soil, the depth of which was 1.5 m. The foundation of the superstructure was made of a pile group with nine piles, and each of them was 0.8 m long. The material, the dimension of the components, the procedure of the PS15S and PS15C tests were exactly the same. Pile foundations and surrounding soil were both designed using the same scale (i.e., 1/15). The test model was shown in Fig. 4 and Fig. 5.

The superstructure and foundation were made of micro-concrete and fine zinc-coated steel bar. Properties of all materials were measured by independent laboratory tests before the shaking table tests. Fig. 6 was typical $G_d/G_0 \sim \gamma_d$ and $D \sim \gamma_d$ curves of the soft soil in the tests, where G_d, G_0, D, γ_d was the dynamic shear modulus, initial shear modulus, damping ratio and shear strain, respectively. Nonlinear properties of soil can be seen clearly in the figure.

As shown in Fig. 4 and Fig. 5, the model tests were instrumented using four types of sensors. Accelerometers (label starting with letter A, AZ and R when located in the superstructure, label starting with letter S when located in the soil), displacement meters, and strain gauges (label starting with letter E) were used to measure the dynamic response of the superstructure, foundation, and soil. Pressure gauges (label starting with letter P) were used to measure the contact pressure between piles and surrounding soil.

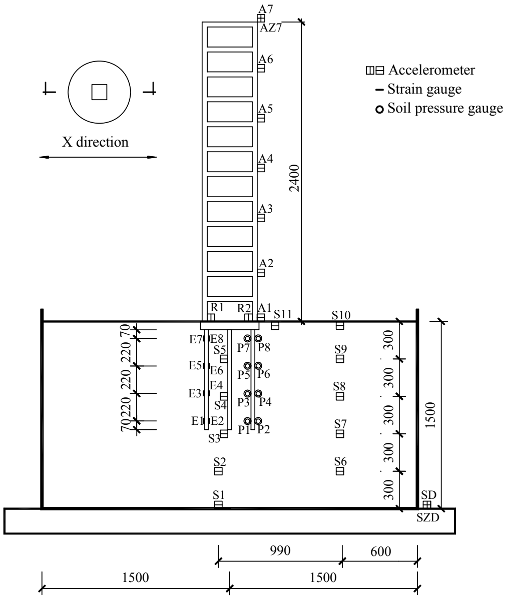

Figure 4. Sketch of the PS15S test model (unit: mm)

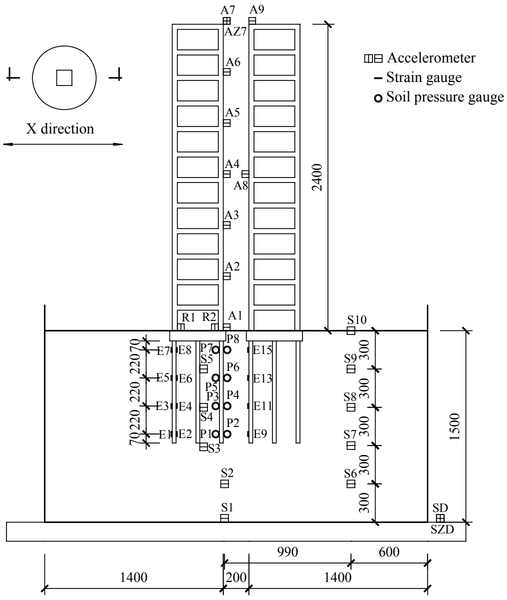

Figure 5. Sketch of the PS15C test model (unit: mm)

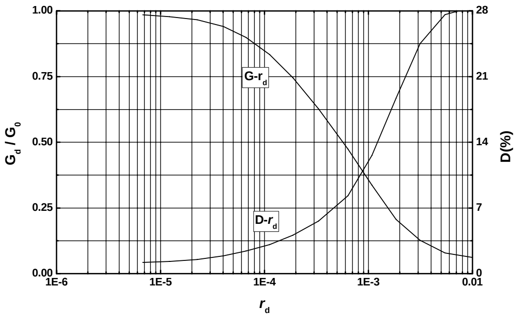

Figure 6. Typical $G_d/G_0 \sim \gamma_d$ and $D \sim \gamma_d$ curves of the soil

2.4 Test Loading Schedule

The El Centro wave and Shanghai bedrock wave were adopted as excitations. The El Centro wave selected for the study was the N-S component from the 1940 El Centro earthquake. The Shanghai bedrock wave was artificial wave for the Shanghai area. Fig. 7 and Fig. 8 show the acceleration time-history and corresponding Fourier spectra of the El Centro Wave and Shanghai bedrock wave. The peak acceleration value was based on the corresponding epicentral intensity according to the seismic code of China, and the peak value and time interval were adjusted according to the similitude relationship. For the sake of conciseness, only the x-directional loading schedule was given in Table 2.

Before and after applying these acceleration levels, the white noise (WN) with small amplitude was applied to the model test to study the corresponding changes in the dynamic characteristics of the system. The input acceleration for the model tests was specified at a time interval equal to 0.002846s, which corresponded to 0.02s according to the prototype scale.

Table 2. Summary of X-direction Test Schedule for the Tests

No.	Excitation	Acceleration Peak Value (g)	
		Prototype	Model
1	EL1, SJ1	0.035	0.115
2	EL2, SJ2	0.1	0.329
3	EL3, SJ3	0.2	0.658
4	EL4, SJ4	0.3	0.988
5	EL5, SJ5	0.4	1.317

Note: (1) EL: El Centro wave; (2) SJ: Shanghai bedrock wave

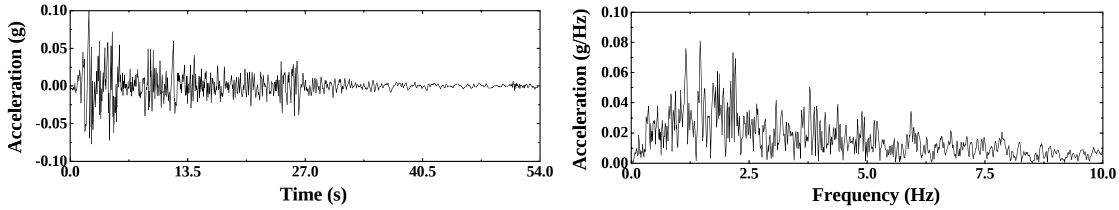

Figure 7. Acceleration time-history and corresponding Fourier spectra of El Centro earthquake

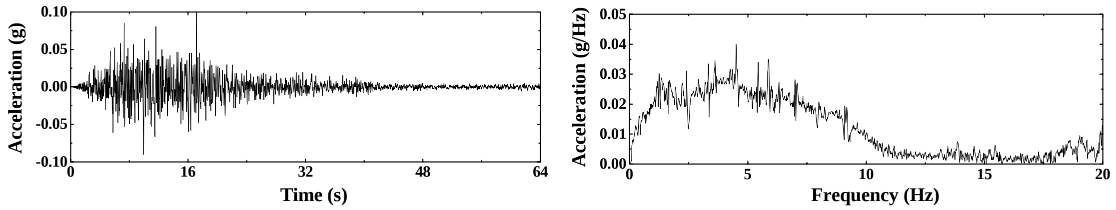

Figure 8. Acceleration time-history and corresponding Fourier spectra of shanghai bedrock wave

3. COMPARISONS OF TESTS PHENOMENA

Compared the test phenomena between the two tests (PS15S and PS15C), several results can be achieved as follows. (1) In the test, the response of the container, soil and superstructure was small when the excitation was small. With the intensity of the excitation increasing, the response of the soil and the structure increased correspondingly. (2) The development mode of the cracks was almost same for the PS15S and PS15C tests. The cracks mainly appeared at the joints of beam-column for the superstructure and the top of the piles at the beginning. With increasing of the excitation, the cracks developed wider and longer. But the width and the number of cracks were different for the two tests. In the PS15S test, it appeared cracks with the width about 0.1 mm at the joints of beam-column after the excitation of SJ5, and there were 1 to 2 horizontal bending cracks appeared at the top of each pile. In the PS15C test, the cracks width at the joints of beam-column was about 0.5 mm after all excitation, and the pile appeared a small number of horizontal bending cracks at the top of each pile. (i.e., the cracks appeared relatively more, wider and earlier in the PS15C test than the PS15C test). (3) The incline degree of the superstructure was different for the two tests. In the PS15S test, it inclined northeastwardly about 0.5 cm and the surface of the soil sank about 1.0 cm after all excitation. In the PS15C test, the superstructure in the west inclined northeastwardly about 1.0 cm and in the east inclined northwestwardly about 1.3 cm after all excitation, and the surface of the soil sank about 2.0 cm. It means that the superstructure in the PS15C test inclined more seriously than that in the PS15S test, and the surface of the soil sank greater in the PS15C test than that in the PS15S test.

4. COMPARISONS OF THE DYNAMIC CHARACTERISTICS

Table 3 shows the frequency and the damping ratio of some of the test stages measured in the PS15S and PS15C tests. As shown in Table 3, because the soil have been strengthened by the two pile foundations in the PS15C test, the soil frequency in the PS15C test was higher than that of the PS15S test. With the increasing of the vibration times and the peak value of the excitation, the frequency of the soil and the interaction system decreased while the damping ratio increased. It was the results of the soil softening, the rigidity degeneration and the crack development of the superstructure and the piles. The frequencies of the interaction system in the two tests were almost same, which indicated the SSSI system had little influence on the first frequency of the interaction system. From Table 3 we can also see that the damping ratios of the interaction system were difference in PS15S and PS15C tests, but the difference was small. It implies that the SSSI system had small influence on the damping of the interaction system.

Table 3. Frequency and Damping Ratio of the Soil and the Interaction System (WN Cases)

Excitation code	Soil frequency (Hz)		Soil damping Ratio (%)		Frequency of interaction system (Hz)		Damping ratio of interaction system (%)	
	PS15S	PS15C	PS15S	PS15C	PS15S	PS15C	PS15S	PS15C
WN1	5.859	6.185	13.28	18.95	3.255	3.255	10.24	11.77
WN2	5.859	5.859	13.88	14.90	3.255	3.255	12.25	8.82
WN3	5.534	5.859	15.81	12.12	2.930	2.930	10.07	10.04
WN4	4.883	5.208	19.46	16.80	2.297	2.297	8.93	10.39
WN5	4.232	5.208	20.36	21.83	1.953	1.953	10.50	9.97
WN6	3.906	4.232	24.58	19.93	1.628	1.628	12.69	12.83

Fig. 9 shows the mode shape curves of the two tests in the WN1 and WN4 cases. Because of the SSI, swing and rocking existed in the superstructure, and it increased while the peak acceleration increased. The main part of the first mode of the superstructure was shear type. All the mode shapes of the two tests were almost similar, which means the SSSI does not change the characteristics of vibration mode. However, the shear characteristic of the mode shape in the PS15C test was more obvious than that in the PS15S test as a result of the relatively more and wider cracks in the PS15C test.

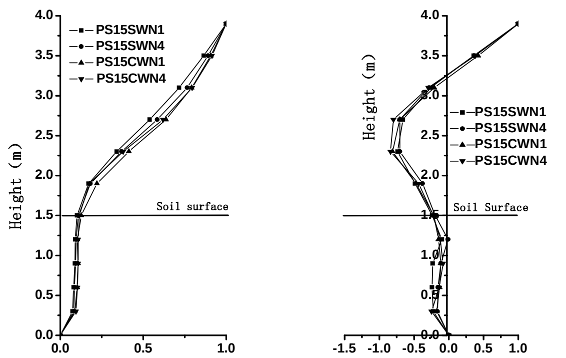

(a) The First Mode (b) The Second Mode

Figure 9. Mode shape curves of the test models (WN1, WN4)

5. COMPARISONS OF THE DYNAMIC RESPONSES

The dynamic responses of the two tests were compared in the following, including the acceleration and displacement of the superstructure, the acceleration of the soil, the strain response of piles, and the contact pressure between the surfaces of the pile-soil of the foundation.

5.1 Comparisons of the Amplification Factors of the Peak Acceleration

The amplification factor was the ratio between the peak acceleration of the measuring points and that of measuring point SD at the container base. As shown in Fig. 10, some rules could be drawn as follows. (1) Magnification or reduction of vibration transferred by the soil was related to the soil characteristic, the excitation magnitude, the spectral characteristics of excitation, and so on. The soil magnified vibration under the small earthquake. However, the soil damped vibration under the strong earthquake because of the non-linear behavior and decline of the stiffness. (2) For the superstructure, the peak acceleration of the floors was obviously different under the small earthquake, which would be explained that the result of the multi-mode response of the structure and the translation and rotation of the foundation. However, under the strong earthquake, the structure response was small because the soil isolated the vibration obviously. (3) The amplification factors of the peak acceleration decreased with the peak acceleration increased. The reason was that the ability of the soil to transfer the vibration weakened with soften and the non-linear of the soil when the inputted excitation intensified and the increasing of times. (4) In the small earthquake, the acceleration of the superstructure in the PS15C test was generally less than that in the PS15S test. On the contrary, that in the PS15C test was generally larger than that in the PS15S test under the strong earthquake. The reason may lie in that the SSSI effect was obvious under the strong earthquake than small earthquake, which would increase the peak acceleration of the superstructure.

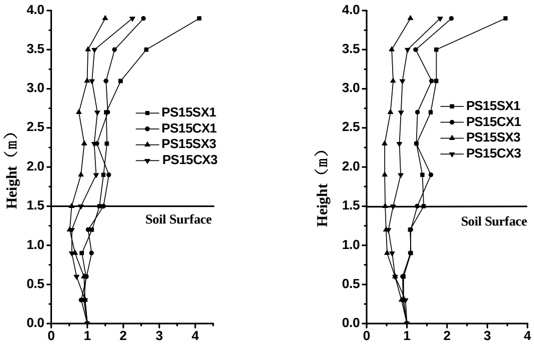

(a) EL1 and EL3 (b) SJ1 and SJ

Figure 10. The amplification factors of the peak acceleration

5.2 Comparisons of the Displacement Response of the Superstructure

As shown in Fig. 11, the peak displacements of the superstructures increased with the peak acceleration of the inputted excitation increased in the two tests. It was the results of the soil softening, the rigidity degeneration of the superstructure and the increase of the translation and rotation of the foundation. Besides, the peak displacement of the superstructure in the PS15C test became smaller than that in the PS15S test, and the tendency became obvious with the increase of the input peak acceleration.

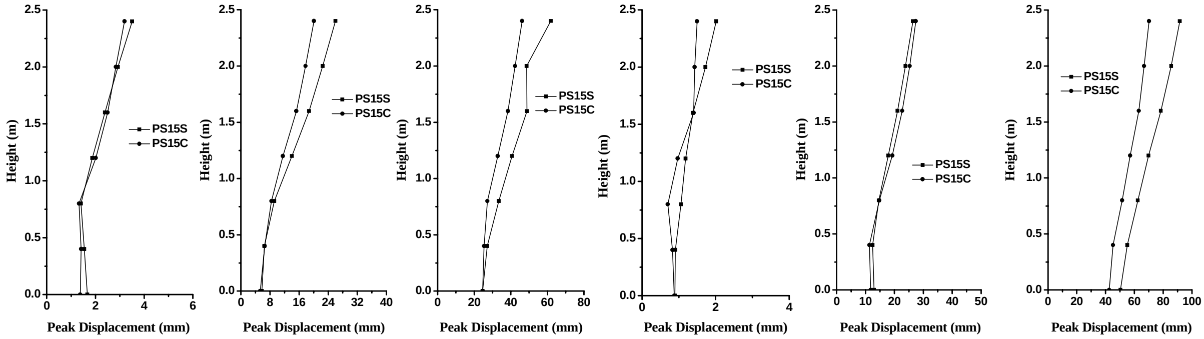

(a) EL1 Case (b) EL3 Case (c) EL5 Case (d) SJ1 Case (e) SJ3 Case (f) SJ5 Case

Figure 11. Comparison of peak displacement of the superstructure

5.3 Comparisons of the Acceleration Response of the Soil

Fig. 12 shows the comparison of the peak acceleration of the soil (Points S1~S5) in the PS15C and the PS15S tests. The measure points S1~S5 in the soil were located in the middle of the container or in the middle piles of the structure. Due to the influence of the SSSI, the peak acceleration of the soil between the piles in the PS15C test was larger than that in the PS15S test. The reason may lie in that the wave was reflected due to the SSSI, therefore the vibration energy of the soil in the SSSI system was increased which could enhanced the acceleration of the soil.

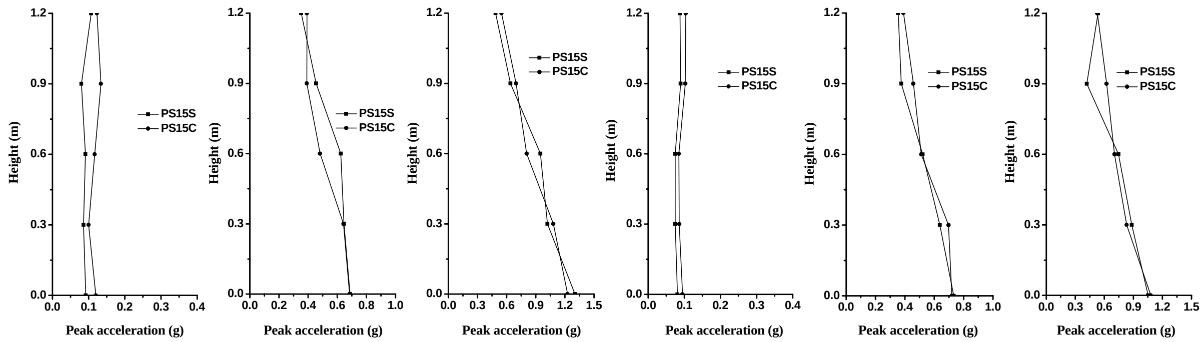

(a) EL1 Case (b) EL3 Case (c) EL5 Case (d) SJ1 Case (e) SJ3 Case (f) SJ5 Case

Figure 12. Comparison of the peak acceleration in the soil

5.4 Comparisons of the Contact Pressure between the Surfaces of the Pile-Soil of the Foundation

Fig. 13 shows the contact pressure between the surfaces of the pile-soil of the foundation in the two tests. In the PS15S test, the contact pressure in the middle of pile was larger than that in the top or bottom of pile, but in the PS15C test, the value of contact pressure in the bottom of pile was more lager than that in the middle or top of the pile when the excitation was strong enough, which implied that the SSSI system had some effect on the contact pressure between the surfaces of the pile-soil of the foundation.

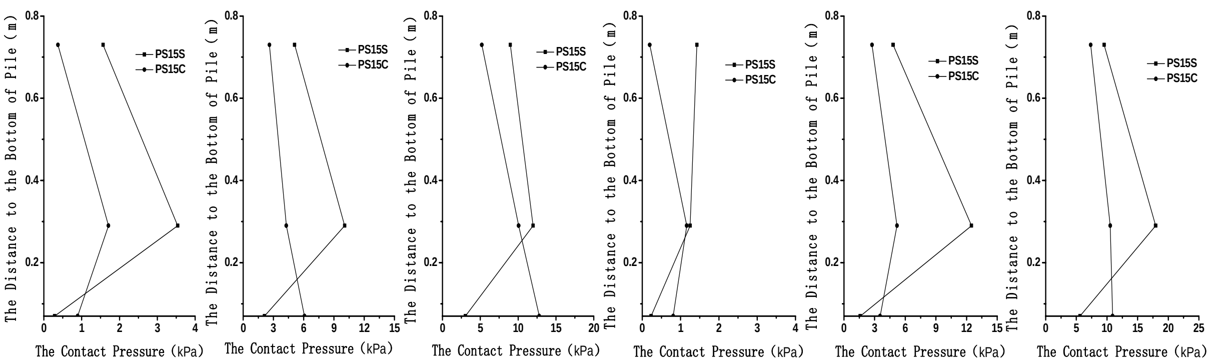

(a) EL1 Case (b) EL3 Case (c) EL5 Case (d) SJ1 Case (e) SJ3 Case (f)SJ5 Case

Figure 13. Comparison of the contact pressure between the surfaces of the pile-soil of the foundation

6. CONCLUSIONS

Shaking table tests on the SSI and SSSI system and the comparisons between the two test results have been conducted. From these studies, the following conclusions were obtained.

(1) The adjacent structures would damage more serious than that in single one.

(2) The SSSI effect have some influence on the soil frequency and the damping ratio of the SSSI system, but have little influence on the frequency and the characteristics of the vibration modes of the SSSI system.

(3) Due to the influence of the SSSI effect, the dynamic response of the SSSI system is different with that of the SSI system. In the small earthquake, the acceleration of superstructure in the SSSI system is generally less than that in the SSI system. While in the strong earthquake, the corresponding response in the SSSI system is generally larger than that in the SSI system. Additionally, the peak displacement of the superstructure in the SSSI system becomes smaller than that in the SSI system, and along with the increase of the input peak acceleration, this tendency becomes obvious.

(4) Owing to the influence of SSSI, the peak acceleration of the soil between the piles in the SSSI system is larger than that in the SSI system.

(5) For the foundation system, the peak contact pressure between the surfaces of the pile-soil was also influenced by the SSSI system.

Through this table shaking test, the dynamic Structure-Soil-Structure Interaction (SSSI) during various excitations is studied. The value of these results lies in improving the seismic design method of structure and giving guidance to the engineering design.

AKCNOWLEDGEMENT

This project was partially supported by the Ministry of Science and Technology of China (Grant No. SLDRCE 09-B-09), the project (Grant No. 51178349) and the key project (Grant No. 90815029 and 51021140006) of the National Natural Science Foundation of China, the key project (Grant No. D09050600370000) of the Beijing Scientific and Technological Program, and the Kwang-Hua Fund for college of Civil Engineering, Tongji University.

REFERENCES

Henry B. Mason, Jonathan D. Bray, Katherine C. Jones, ZhiQiang Chen, Tara C. Hutchinson, Nicholas W. Trombetta, Benjamin Y. Choy, Bruce L. Kutter, Gregg L. Fiegel, Jack Montgomery, Roshani J.Patel, Robert D. Reitherman, Chandrakanth Bolisetti, Andrew S. Whittaker. (2010). Earthquake input motions and seismic site response in a centrifuge test examining SFSI effects. *Fifth international conference on recent advances in geotechnical earthquake engineering and soil dynamics and symposium in honour of professor I. Midriss*. Paper No. 5.48a.

Bard, P. Y., Chazdlas, J. L., Guéguen, P., et al. (2006). Site-city interaction. *Geotechnical, Geological, and Earthquake Engineering*. **2:1**, 91-114.

Broc, D. (2006). Soil structure interaction: theoretical and experimental results. *ASME Pressure Vessels and Piping Division Conference (PVP2006/ICPVT-11): Pressure Vessel Technologies for the Global Community*. Vancouver, British Columbia, Canada, 886-891.

Celebi, M. (1993a). Seismic responses of two adjacent buildings I: Data and analyses. *Journal of Structural Engineering, ASCE*. **119:8**, 2461-2476.

Celebi, M. (1993b). Seismic responses of two adjacent buildings II: Interaction. *Journal of Structural Engineering, ASCE*. **119:8**, 2477-2492.

Ghergu, M. and Ionescu, I. R. (2009). Structure-soil-structure coupling in seismic excitation and city effect. *International Journal of Engineering Science*. **47**, 342-354.

Groby, J., Tsogka, C. and Wirgin, A. (2005). Simulation of seismic response in a city-like environment. *Soil Dynamics and Earthquake Engineering*. **25: (7-10)**, 487-504.

Gueguen, P., Bard, P., et al. (2002). Site-city seismic interaction in Mexico city-like environments an analytical study. *Bulletin of the Seismological Society of America*. **92:2**, 794-811.

Karabalis, D. L. and Mohammadi, M. (1998). 3-d dynamic foundation-soil-foundation interaction on layered soil. *Soil Dynamics and Earthquake Engineering*. **:17**, 139-152.

Kham, M., Semblat, J. F. Bard, P. Y., et al. (2006). Seismic site-city interaction: main governing phenomena through simplified numerical models. *Bulletin of the Seismological Society of America*. **96:5**, 1934-1951.

Kitada, Y., Hirotani, T. and Iguchi, M. (1999). Models test on dynamic structure-structure interaction of nuclear

power plant buildings. *Nuclear Engineering and Design*. **192: (2-3)**, 205-216.
Lehmann, L. and Antes, H. (2001). Dynamic structure-soil-structure interaction applying the symmetric Galerkin boundary method (SGBEM). *Mechanics Research Communications*. **28:3**, 297-304.
Li, P. Z., Ren, H. M., Lu, X. L., et al. (2008). Shaking table tests of dynamic interaction of soil-structure considering soil liquefaction. *14th World Conference on Earthquake Engineering*. Paper No. 04-01-0024.
Lu, X. L., Chen, Y. Q., Chen, B. and Li, P. Z. (2002a). Shaking table model test on dynamic soil-structure interaction system. *Journal of Asian Architecture and Building Engineering*. **1:1**, 55-64.
Lu, X. L., Li, P. Z., Chen, B. and Chen, Y. Q. (2002b). Numerical analysis of dynamic soil-box foundation-structure interaction system. *Journal of Asian Architecture and Building Engineering*. **1:2**, 9-14.
Lu, X.L., Li, P.Z., Chen, B. and Chen, Y.Q. (2005). Computer simulation of the dynamic layered soil-pile-structure interaction system. *Canadian Geotechnical Journal*. **42:3**, 742-751.
Mizuno, H. (1980). Effects of structure-soil-structure interaction during various excitations. *7th World Conference on Earthquake Engineering*. 149-156.
Nakagawa, S., Kuno, M., Naito, Y., et al. (1998). Forced vibration tests and simulation analyses of a nuclear reactor building. *Nuclear Engineering and Design*. **179:2**, 145-156.
Padron, L. A., Aznarez, J. J. and Maeso, O. (2009). Dynamic structure-soil-structure interaction between nearby piled buildings under seismic excitation by BEM-FEM model. *Soil dynamics and earthquake engineering*. **9:6**, 1084-1096.
Qian, J. and Beskos, D. E. (1995). Dynamic interaction between 3-d rigid surface foundations and comparison with the ATC-3 provisions. *Earthquake Engineering and Structural Dynamics*. **24:3**, 419-437.
Qian, J. and Beskos, D. E. (1996). Harmonic wave response of two 3-d rigid surface foundations. *Soil Dynamics and Earthquake Engineering*. **:15**, 95-110.
Semblat, J., Kham, M. and Bard, P. (2008). Seismic-wave propagation in alluvial basins and influence of site-city interaction. *Bulletin of the Seismological Society of America*. **98:6**, 2665-2678.
Xu, J., Costantino, C., Hofmayer, C., et al. (2004). Seismic response prediction of NUPEC's field model tests of NPP structures with adjacent building effect. *ASME/JSME Pressure Vessels and Piping Conference*. 1-11.
Yahyai, M., Mirtaheri, M. and Mahoutian, M. et al. (2008). Soil structure interaction between two adjacent buildings under earthquake load. *American Journal of Engineering and Applied Sciences*. **1:2**, 121-125.